

Three-Dimensional Analysis of Scoliosis Surgery Using Stereophotogrammetry

Kellogg S. Booth, Stanley B. Jang, Chris W. Reilly, Bonita J. Sawatzky and Stephen J. Tredwell

*Department of Computer Science, University of British Columbia
Department of Orthopaedics, B.C. Children's Hospital
Vancouver, British Columbia, Canada*

ABSTRACT

Scoliosis is a deformity characterized by coronal, sagittal and axial rotation of the spine. Surgical instrumentation (metal pins and rods) and eventual fusion of the spine are required in severe cases. Assessment of the deformity requires enough accuracy to allow proactive planning of individual interventions or implant designs. Conventional 2-D radiography and even 3-D CT scanning do not provide this, but our new stereophotogrammetric analysis and 3-D visualization tools do. Stereophoto pairs taken at each stage of the operation and robust statistical techniques can be used to determine rotation, translation, goodness of fit, and overall spinal contour before, during and after the surgical instrumentation.

Novel features of our software include 3-D digitizing software that improves existing stereophotogrammetry methods, robust statistical methods for measuring 3-D deformity and estimating errors, full 3-D visualization of spinal deformities with optional head-coupled stereo ("fish tank virtual reality"), full integration with commercial animation software, use of consumer PhotoCD technology that significantly lowers costs for data collection and storage while increasing accuracy, and simultaneous 3-D viewing and control at remote locations over high-speed ATM networks.

1 INTRODUCTION

Scoliosis is a three-dimensional deformity of the spine, characterized by rotations in all three planes of view. In the posterior view, the spine is an “S” curve as opposed to a vertical column in a normal spine. In the lateral view, a normal spine would be an “S” curve whereas the scoliotic spine is fairly straight. In the axial view (from the head looking down), some of the vertebrae are twisted about the spinal axis. Figure 1 illustrates both the scoliotic and normal spines in the three views. Scoliosis is a common problem among children and adults. There are a variety of different types of scoliosis. The curve may develop, secondary to a neuromuscular disorder such as spina bifida or cerebral palsy, or it may be congenital, due to an underlying abnormality of the formation of the spine. In many cases no cause of the scoliosis can be determined. This is commonly termed idiopathic scoliosis.

Progression or worsening of the scoliotic curve can result in serious compromises in pulmonary and cardiac function. In the idiopathic group, non-operative treatment using braces is often successful. However, approximately 20% of the patients with scoliosis requiring treatment will undergo surgical intervention. The most radical intervention is spinal fusion in which the vertebrae are forced to grow together by the application of bone chips and marrow to the vertebrae. Spinal fusion stops the progression of a curve that may lead to debilitating back problems, compromised pulmonary and cardiac function, and a gross cosmetic deformity in adulthood. Surgical spinal instrumentation systems, consisting of metal pins and rods that are inserted into the vertebrae, are required to achieve predictable fusion of the spine. These are used to correct the scoliosis towards a more normal spinal contour.

The cosmetic deformity is caused by the adaptation of the rib cage, so that on the convex side of the curve a prominent rib hump develops. This deformity can be measured clinically using a special level device, called a scoliometer, which is placed on the back as the patient flexes forward. This measurement describes the clinical rib hump deformity. The rib hump is thought to be due to vertebral rotation (twisting).

In the past 25 years the surgical management of spinal deformities has undergone tremendous change. Modern



a) normal - lateral



b) normal - posterior



c) normal - axial



d) scoliosis - lateral



e) scoliosis - posterior



f) scoliosis - axial

Figure 1: The lateral, posterior and axial views of a portion of a normal and a scoliotic spine.

spinal instrumentation systems have provided lasting correction of the sagittal (lateral) and coronal (posterior) spinal deformity present in idiopathic scoliosis. The surgical procedure for instrumentation involves securing hooks onto strategic vertebrae, correcting the shape and orientation of the spine, stabilizing that position by clamping stainless steel rods to the hooks, and finally, fusing the spine. Fusion is accomplished by placing bone graft and bone marrow obtained from the patient's hip between the vertebrae.

Recently developed systems, such as Cotrel-Dubousset instrumentation, have attempted to address all of the components of the scoliotic deformity, including the axial rotational deformity. This is of importance because it is believed that the rib hump deformity described earlier is caused by twisting in the vertebrae. However, accurate measurement of three-dimensional changes produced by spinal instrumentation has yet to be achieved and debate continues regarding axial rotation changes. It remains unclear whether current instrumentation techniques do establish true vertebral derotation or if they merely result in pure translation of the vertebral column. There have been a number of approaches to accurately assess the rotational and translational changes in the vertebrae.

In the next two sections we review previous techniques for analyzing scoliosis deformities and then introduce our new techniques by summarizing the five major steps: image acquisition, stereo digitization, computation of vertebral movement, statistical analysis of the results, and determination of the plane of maximal deformity. Following that, we discuss the novel aspects of our work in terms of the computer graphics techniques that are employed during the various steps: interactive stereographic digitizing, full 3-D visualization and description of curvature, integration of our software with commercial animation packages to produce "professional quality" visualization suitable for communication and dissemination of results, and multi-user extensions to support collaborative use of the new tools across both normal and high-speed ATM networks.

2 PREVIOUS ANALYSIS TECHNIQUES

Many techniques have been applied to define the three-dimensional spinal anatomy in idiopathic scoliosis. Some of these techniques have been applied pre- and post-operatively in an attempt to quantify the effect of spinal instrumentation. A method of rotational assessment using plain anterior-posterior radiographs with a torsionmeter was developed by Nash and Moe. This system has been assessed and found to be unacceptable for the clinical assessment of vertebral rotation³. Drerup modified the plain radiographic technique by using standard vertebral parameters to relate pedicle position and rotation to the estimated center of the vertebral body⁶. This improved the accuracy of the plain radiographic technique with a reported standard deviation of five degrees. Drerup's technique and three similar methods have been compared using an isolated single vertebrae rotated by fixed angles in a bench study. Mean error was of a similar magnitude¹⁰. The technique has not been used successfully to define rotational correction in post-operative patients.

CT scanning has been widely used in an attempt to compare pre- and post-operative vertebral position. The usual technique uses single slices through the spinal segment being assessed. A difficulty with the technique has been a lack of a standard reference frame to control for changes in gantry positioning pre- and post-operatively. Vertebral rotation has also been assessed segmentally utilizing CT cuts along the entire spinal axis and measuring post-operative segmental de-rotation¹¹. Studies using both techniques have produced results with marginal accuracy. Lack of a standard reference frame between pre- and post-operative studies compounds this problem. CT scanning techniques are also limited due to the radiation exposure, which prevents routine three-dimensional reconstructions of scoliotic patients. The presence of the post-operative metal instrumentation also causes significant image artifacts in both single slice and three-dimensional reconstructions.

Many investigators have utilized stereoradiographic techniques to accurately measure the three-dimensional anatomy of the scoliotic spine². These systems commonly use conventional anterior-posterior and a 20-degree caudal tilted

view or a 50-degree oblique projection. They rely on stereo digitization of radiographic features of the vertebrae to produce 3-D coordinates. The technique is limited due to the inherent inaccuracy produced in selecting radiographic landmarks leading to reconstruction errors of up to 5mm for translation values ¹. In post-operative patients, landmark identification is more difficult due to the presence of the instrumentation and bone graft. This limits the ability of the technique to quantify the amount of de-rotation expected.

The presence of the metallic spinal instrumentation, the complex three-dimensional scoliotic deformity and the changes in vertebral anatomy seen in scoliosis have made accurate measurement difficult. Current techniques do not conclusively define vertebral de-rotation that is theoretically produced with systems such as Cotrel-Dubousset instrumentation. Moreover, intra-operative changes created during the distraction and rotation phases of Cotrel-Dubousset instrumentation have not been assessed by other investigators. Our goal was to develop measurement and visualization tools that would overcome these limitations.

3 STEREOPHOTOGRAMMETRIC ANALYSIS OF SCOLIOSIS

A system of stereophotogrammetric analysis has been developed to allow accurate 3-D assessment of the scoliotic spine during spinal instrumentation. Stereophoto pairs are taken at sequential phases of the operative procedure. These 35 mm slides are digitized using Kodak's Consumer PhotoCD service. Multiple data points collected from the stereo images allow the calculation of 3-D positions for the vertebrae at each stage of the procedure. Statistical techniques are employed to provide a measure of the robustness of the results. These results allow the surgeons to gain a better understanding of the effects of each step in the surgical procedure.

3.1 Image Acquisition

Overhead intra-operative photography is used to obtain stereo photographs during posterior spinal instrumentation procedures in idiopathic scoliotic patients. A retractable overhead boom with a pair of 35 mm cameras equipped with fixed focal length calibrated lenses and synchronous flash was constructed for this purpose. The lenses of the cameras are approximately parallel and the distance between their focal points is approximately 20 cm. Photograph quality is enhanced through the use of high quality 60 ASA film. A metal target frame of known size with fixed calibration targets was fabricated to facilitate calculation of the camera parameters. It can be sterilized and placed so that it frames the operative field during intra-operative photography. A metal ruler, fixed intra-operatively over the posterior superior iliac spines using a clear adhesive drape, is utilized in data analysis as an internal reference for pelvic position and thus eliminates error created by patient or camera motion.

The stereophotogrammetric technique involves initial set up prior to draping followed by boom/camera storage in the operating room during the procedure. At specific points during the operative procedure the boom is positioned over the patient and aligned with previously placed floor marks through the use of three pins ensuring accurate position. This positioning of the boom is strictly for the purposes of achieving the correct field of view in the photographs, and not for attempting to place the patient's spine in the same relative location as previous photographs. Simultaneous photographic pairs are then taken at the following operative stages: 1) exposure, 2) Harrington spreader in place, 3) concave rod in, 4) concave rod rotated, 4) concave rod rotated and distracted, and 5) convex rod in.

The 35 mm slides are transferred onto Kodak Consumer PhotoCD's, providing a digital representation of the slides. These images are of a sufficiently high resolution, 2048x3072 pixels, to accommodate stereo digitization on a computer workstation. Besides being an economical method for converting photographic slides into a digital format, the PhotoCD's are a convenient and secure form of media for archiving the data. Each read-only compact disc is capable of storing one hundred images.

In addition to the Consumer PhotoCD, Kodak produces two higher quality PhotoCD's intended for industrial use. These are the Professional and the Diagnostic PhotoCD's. One set of patient data has been digitized onto Kodak's Professional CD. This CD boasts higher quality and higher resolution than the Consumer CD. The maximum resolution is double that of the Consumer CD in each direction, resulting in images that are 4096x6144 pixels. After studying the one case using this CD format, there does appear to be some potential for better accuracy over the Consumer CD. The drawbacks, however, are higher cost and awkwardness in working with 75 megabyte files. Because the accuracy obtained with the Consumer CD seems adequate for our current needs, they will continue to be used. If more accuracy is required in the future, the Professional CD's may be reconsidered.

3.2 Stereo Digitization

Each image collected from the operation provides a view of the patient's spine, the reference ruler, and the calibrated frame. The objects of interest for analysis are the individual exposed vertebrae. Each vertebra is a rigid body with the potential to move relative to the other vertebrae. The goal during stereo digitization is to collect enough data on the surface of each exposed vertebra so that the movement of the vertebrae can be determined between successive stages in the operation.

Current stereophotogrammetric techniques employ large stereoplotters (sometimes connected to computers) to digitize aerial photographs. A trained technician views these photographs stereoscopically with the stereoplotter and determines 3-D coordinates for landmarks in view in both photographs. Our images are digitized by our research group using custom software developed by our group specifically for this project. The software, which runs on Silicon Graphics computer workstations, enables a user to interactively stereo digitize two pairs of stereo images simultaneously. Sub-images of each of the four images are displayed on the computer monitor and each can be zoomed and panned. Although the computer workstation is stereo-capable, and the software does allow for digitization while viewing in stereoscopic mode, we typically work with the images separately (side-by-side).

To stereo digitize a landmark visible in both images, the user selects the desired point in one image, then specifies a region in a second image for the software to search for the corresponding point. The user may override this auto-matching feature and choose the matching point in the second image manually. The “messiness” of these intra-operative images make it very difficult to increase the amount of computer automation in the stereo digitization process.

The accuracy of digitized landmarks on a vertebra can be verified at any time with the software by comparing their relative positions to the same landmarks in a previously digitized stereo pair. The user can examine the differences in distances between points in the two stages both numerically and visually, by interactively viewing the 3-D data for the two stages in the same 3-D coordinate system. This feature is particularly useful because landmarks of insufficient accuracy can be deleted and replaced during the stereo digitization process. Statistics can be computed on the vertebral data to determine if the vertebral rotation and translation results have the necessary accuracy (these statistical calculations are explained later). If the necessary accuracy is not obtained, more landmarks may be digitized before proceeding with the stereo digitization of the next vertebra.

There are fewer landmarks to choose from in the photos of the later stages of the operation because of the instrumentation already in place, and because parts of some of the vertebrae are often chipped off during the operation. Typically, landmarks found in the last stage of the operation, when all of the surgical implants are in place, are visible in all of the previous stages. Thus, stereo digitization usually begins with the last stage and proceeds backwards in time. As many as ten points are digitized for each fully exposed vertebra, although only three points are necessary to mathematically determine the position and orientation of a single vertebrae. Digitizing redundant points allows for increased accuracy in the statistical calculations.

After this process has been completed, 3-D “camera” coordinates are calculated from the 2-D “image” coordinates of the landmarks. The calibration frame, which is in view in each of the images, contains known 3-D landmarks. This information is used to calculate the two cameras’ exterior orientation parameters (position and orientation of the cameras) ¹². Given these parameters and the 2-D image coordinates, 3-D coordinates for the landmarks are computed

using a least squares fit.

3.3 Computation of Vertebral Movement

The 3-D data from the sets of stereo images consist of the camera coordinates of landmark points on each vertebra at each stage of the operation. Before computing translations and rotations of the vertebrae from this data, the coordinates must be converted to a “patient” coordinate system. This is accomplished with the aid of a metal ruler taped to the patient’s skin just above the pelvis. This ruler is considered fixed relative to the pelvis. The data from each of the stages is converted so that the ruler is aligned in each of the slides, putting all of the data points in the same coordinate system.

The change in position of each vertebra between any two stages can be computed from the data. The most interesting result for analyzing the success of the operation is the transformation between the first stage of the operation (initial surgical exposure of spine) and the last stage (the end of surgery just prior to closing the incision). Transformations between intermediate stages are relevant for studying the assumptions underlying the surgical procedure.

The calculation of the movement of a vertebra between two stages is equivalent to the calculation of an affine transformation between two similarly shaped clouds of 3-D point data. Ideally, the two sets of points for a single vertebra form a rigid object, subject only to translation and rotation in space. But of course there is error in the data that must be taken into account. Translations are computed from the center of mass of the data points and are stated as x , y , and z axis displacements. These correspond to the best least squares translation for the data.

Vertebral rotations are computed by finding the rotation matrix that best matches the corresponding data points for the vertebra between the two stages. The rotation matrix is calculated using a linearized iterative least squares algorithm. This algorithm converges on the rotation values given that suitable initial estimates are chosen. The initial estimate is computed by the solution of an “orthogonal Procrustes problem”⁸. A minimum of three points is necessary to perform

these calculations. The problem is under-determined if there are fewer than three points and over-determined if there are more.

The “orthogonal Procrustes problem” explores the possibility that one subspace may be rotated exactly into another. It is stated formally as follows.

$$\text{minimize } \| A - BQ \|_F$$

subject to the constraint that $Q^t Q = I$,

where A and B are the $n \times 3$ data matrices specifying the two stages of vertebral data and

Q is an unknown 3×3 rotation matrix.

The solution calculates the rotation matrix Q that satisfies the equation and the constraints using the Frobenius norm as the error metric⁹. The algorithm to compute Q is as follows.

1. Let $C = B^t A$
2. Compute the singular value decomposition (SVD) $U^t C V$
3. Then $Q = UV^t$

This algorithm generates a suitable initial estimate of the rotation of the vertebrae. It is not appropriate as a final result for two reasons. First, the algorithm is not actually searching for a rotation matrix Q , but for an orthogonal matrix Q . An orthogonal matrix has a determinant of ± 1 . A rotation matrix has a determinant of 1. A matrix with a determinant of -1 is a reflection matrix. Our data will occasionally produce a reflection matrix if there is significant error in the data or if the data is highly symmetric. The second problem with the algorithm is that translation of the data is not dealt with. Before this algorithm is used to generate a rotation matrix from the data, we translate the data from one stage so that the center of masses of the two stages of data coincide. This translation does not produce the minimum error value using the Frobenius norm, but it is very close.

The linearized iterative least squares algorithm uses the results of Procrustes’ algorithm as an initial estimate in solving for the rotation matrix. Least squares is frequently used to solve problems that can be described by a system of linear

equations and contain some error. However, the system of equations that are derived for this problem are non-linear. The equations are linearized using Taylor's Theorem and must be solved iteratively.

The algorithm is derived as follows.

1. A point is at location $a = (a_x, a_y, a_z)$ in one stage and moves to location $a' = (a'_x, a'_y, a'_z)$ in a later stage.
2. Then $a' = aM$ where M is the 4×4 transformation matrix that maps the two stages of data.

Many of the elements of M are non-linear with respect to the original data. This matrix can be viewed as the product of three rotation matrices about the coordinate axes R_x , R_y and R_z (with respective rotation amounts r_x , r_y , and r_z), and a translation matrix T .

$$\begin{aligned}
 M &= \begin{pmatrix} m_{11} & m_{12} & m_{13} & 0 \\ m_{21} & m_{22} & m_{23} & 0 \\ m_{31} & m_{32} & m_{33} & 0 \\ m_{41} & m_{42} & m_{43} & 1 \end{pmatrix} \\
 &= R_x R_y R_z T \\
 &= \begin{pmatrix} c_y c_z & c_y s_z & -s_y & 0 \\ s_x s_y c_z - c_x s_z & s_x s_y s_z + c_x c_z & s_x c_y & 0 \\ c_x s_y c_z + s_x s_z & c_x s_y s_z - s_x c_z & c_x c_y & 0 \\ x & y & z & 1 \end{pmatrix}
 \end{aligned}$$

where

$$c_x = \cos(r_x)$$

$$c_y = \cos(r_y)$$

$$c_z = \cos(r_z)$$

$$s_x = \sin(r_x)$$

$$s_y = \sin(r_y)$$

$$s_z = \sin(r_z)$$

x = translation along the x -axis

y = translation along the y -axis

z = translation along the z -axis

Expanding on the relationship between a' , a and M , the following three equations result.

$$a'_x = m_{11}a_x + m_{21}a_y + m_{31}a_z + m_{41}$$

$$a'_y = m_{12}a_x + m_{22}a_y + m_{32}a_z + m_{42}$$

$$a'_z = m_{13}a_x + m_{23}a_y + m_{33}a_z + m_{43}$$

From these equations, we can define three objective functions F , G and H .

$$F = 0 = m_{11}a_x + m_{21}a_y + m_{31}a_z + m_{41} - a'_x$$

$$G = 0 = m_{12}a_x + m_{22}a_y + m_{32}a_z + m_{42} - a'_y$$

$$H = 0 = m_{13}a_x + m_{23}a_y + m_{33}a_z + m_{43} - a'_z$$

Each of these equations is non-linear because of the elements from the matrix M . These equations may be linearized using Taylor's theorem.

$$0 = (F)_0 + \left(\frac{\partial F}{\partial r_x}\right)_0 dr_x + \left(\frac{\partial F}{\partial r_y}\right)_0 dr_y + \left(\frac{\partial F}{\partial r_z}\right)_0 dr_z + \left(\frac{\partial F}{\partial x}\right)_0 dx + \left(\frac{\partial F}{\partial y}\right)_0 dy + \left(\frac{\partial F}{\partial z}\right)_0 dz$$

$$0 = (G)_0 + \left(\frac{\partial G}{\partial r_x}\right)_0 dr_x + \left(\frac{\partial G}{\partial r_y}\right)_0 dr_y + \left(\frac{\partial G}{\partial r_z}\right)_0 dr_z + \left(\frac{\partial G}{\partial x}\right)_0 dx + \left(\frac{\partial G}{\partial y}\right)_0 dy + \left(\frac{\partial G}{\partial z}\right)_0 dz$$

$$0 = (H)_0 + \left(\frac{\partial H}{\partial r_x}\right)_0 dr_x + \left(\frac{\partial H}{\partial r_y}\right)_0 dr_y + \left(\frac{\partial H}{\partial r_z}\right)_0 dr_z + \left(\frac{\partial H}{\partial x}\right)_0 dx + \left(\frac{\partial H}{\partial y}\right)_0 dy + \left(\frac{\partial H}{\partial z}\right)_0 dz$$

where,

$$(F)_0 = a_x c_y c_z + a_y (s_x s_y c_z - c_x s_z) + a_x (c_x s_y c_z + s_x s_z) + x - a'_x$$

$$\left(\frac{\partial F}{\partial r_x}\right)_0 = a_y c_x s_y c_z + a_y s_x s_z - a_z s_x s_y c_z + a_z c_x s_z$$

$$\left(\frac{\partial F}{\partial r_y}\right)_0 = -a_x s_y c_z + a_y s_x c_y c_z + a_z c_x c_y c_z$$

$$\left(\frac{\partial F}{\partial r_z}\right)_0 = -a_x + c_y s_z - a_y s_x s_y s_z - a_y c_x c_z - a_z c_x s_y s_z + a_z s_x c_z$$

$$\left(\frac{\partial F}{\partial x}\right)_0 = 1$$

$$\left(\frac{\partial F}{\partial y}\right)_0 = 0$$

$$\left(\frac{\partial F}{\partial z}\right)_0 = 0$$

Simplifying the three linearized equations yields the following system of equations.

$$0 = m_{11}a_x + m_{21}a_y + m_{31}a_z + x - a'_x + (m_{31}a_y - m_{21}a_z)dr_x + (-a_x s_y c_z + a_y s_x c_y c_z +$$

$$a_z c_x c_y c_z)dr_y + (-m_{12}a_x - m_{22}a_y - m_{32}a_z)dr_z + dx$$

$$0 = m_{12}a_x + m_{22}a_y + m_{32}a_z + y - a'_y + (m_{32}a_y - m_{22}a_z)dr_x + (-a_x s_y s_z + a_y s_x c_y s_z +$$

$$a_z c_x c_y s_z)dr_y + (m_{11}a_x + m_{21}a_y + m_{31}a_z)dr_z + dy$$

$$0 = m_{13}a_x + m_{23}a_y + m_{33}a_z + z - a'_z + (m_{33}a_y - m_{23}a_z)dr_x + (-a_x c_y - a_y s_x s_y -$$

$$a_z c_x s_y)dr_y + dz$$

For these equations, $a_x, a_y, a_z, a'_x, a'_y$ and a'_z are known data values. The elements of the matrix $M=(m_{ij})$, including x, y and z , and the sin and cos values are calculated from the initial approximations r_x, r_y, r_z, x, y and z . This leaves the six unknown corrections: dr_x, dr_y, dr_z, dx, dy and dz . On the first iteration in solving this system of three equations, initial approximations are used to solve for the unknown corrections. These corrections are then added to the approximations and these revised estimates are used on the second iteration of solving the system of equations. This process continues until a satisfactory level of accuracy is acquired.

3.4 Statistical Analysis of the Results

Estimates of the error in our computation of the position and orientation for each vertebra are computed for the data to give some indication of the accuracy of our results.

An estimate of the standard deviation of the raw 3-D data for each vertebra, generated by the digitization software, is calculated first. Because this data was obtained from stereophotogrammetry, its accuracy along different directions varies. Depth, the distance from the camera, is less accurate. However, at this time, only a single measure of standard deviation is used. This value, s , depends on the fit of the data between two stages and the number of data points available on the vertebra in the two stages.

1. Let A and B be $n \times 3$ data matrices specifying the two stages of vertebral data
2. Let Q be the 3×3 rotation matrix calculated to transform matrix A into B .
3. Then $s^2 = \frac{\|A - BQ\|_F}{6(n-1)}$

The error estimate for the vertebral rotation results is computed using a statistical resampling technique known as “bootstrapping”⁷. This technique involves perturbing the raw vertebral data by a random Gaussian displacement with standard deviation s as computed above, then recalculating the vertebral rotations with the perturbed data. This process is repeated many times, providing a sample of vertebral rotation results. Standard deviations for these sets of rotations are calculated to represent the error estimates for the rotation of each vertebra. The bootstrapping technique is simple, yet accurate, assuming only that the sample standard deviations for the original data are accurate and that a sufficient number of samples are taken when the bootstrapping is performed.

The error estimates for the translation results are computed directly by taking the difference between the center of masses of two stages of vertebral data. If the standard deviation of the center of mass is s , the standard deviation of the difference of two centers of mass is $2s$.

Using the vertebral translation and rotation data, various hypotheses can be tested. These include questions about

choices in the hardware for instrumentation, choices in the implementation of the instrumentation during surgery and the underlying changes in the anatomy due to surgical correction. The hypotheses are tested using standard statistical tools such as the t-test and ANOVA. The bootstrapping technique provides a measure of the accuracy of this data. Our techniques produce data at least as reliable as that reported in other studies in the literature, and sometimes more accurate by a factor of two based on comparison of our error estimates with the error estimates reported in the literature.

3.5 Determination of the Plane of Maximal Deformity

One study that is currently being conducted is the change in the “plane of maximal deformity” in the spine during and after surgical intervention. The maximal deformity is the primary curve in the scoliotic spine, consisting of about seven vertebrae. The orientation of this curve can be described by the plane in which it lies. Instead of attempting to straighten this curve, modern instrumentation systems attempt to re-orient the curve so that the plane lies strictly in the lateral view (i.e. the curve is not visible in the posterior view). This is how a normal spine is shaped.

Using the vertebral data collected, the change in orientation of the plane of maximal deformity between stages in surgery can be determined. These results are a vast improvement from the qualitative assessment of post-operative radiographs that surgeons are currently using to track the plane of maximal deformity. Until now, a quantitative study of this property of the scoliotic spine has not been possible.

4 VISUALIZATION

This work makes a number of advances in the application of computer graphics to surgery and therapeutic procedures. We discuss each of these in turn in this section and suggest additional research that could further enhance our techniques.

4.1 Interactive Stereographic Digitizing

The new stereographic digitizing software that has been developed provides semi-automated point matching based on stereo correlation techniques derived from algorithms developed in the field of computer vision ⁴. Traditional stereophotogrammetry is essentially a manual process, relying on the skill of the operator to assess relative depths of features in the two stereo fields. Our software uses local search techniques that compare the digital RGB intensity values to find a local minimum in the difference between the landmark and the target.

We currently do not take into account differences in intensity due to specular reflection caused by the difference in viewing angles between the two cameras because we have not found this to be necessary. A more robust matching algorithm would incorporate this capability.

A related, more difficult problem is the difference in RGB intensity between two sets of stereo pairs. Because the images are taken at different times during the operation, not only are the camera and lighting angles different, the vertebrae themselves are different because of the varying amounts of fluid (blood and saline solution) that are present. In practice this is more of a problem, but not one we have had time to deal with adequately.

4.2 Full 3-D Visualization and Description of Curvature

The medical literature on scoliosis frequently reports curvature and changes in curvature solely based on 2-D projections, such as the often-used Cobb angle ⁵. This is an artifact of using planar radiographs. Our software provides true 3-D viewing from arbitrary viewpoints, thus facilitating both quantitative 3-D curvature information and interactive exploratory analysis of the 3-D shape of the spine. This allows us to measure the deformity as a 3-D displacement and rotation, rather than as a rotation in a 2-D projection of the data.

Our stereo digitization supports a stereo viewing mode using LCD shutter lenses. Full head-coupled stereo viewing

(“fish tank virtual reality”) is available for the vertebral models produced by the software using the LCDS shutter lenses and a 6-D head tracking device.

4.3 Integration with Commercial Animation Packages

Rather than write our own animation software, we used commercial 3-D modeling software to produce animations of the surgical correction of a patient’s spine. This is accomplished by importing the digitized data into the modeler along with a “standard” polygonal model of a human spine obtained commercially. The model spine was scaled to fit the data and each vertebra is translated and rotated to match the pre-operative position of the patient’s corresponding vertebra. Animation channels are generated from the translations and rotations computed from the data and these are applied to the modified model vertebrae. The model spine can then be animated with lighting and shading to illustrate the initial position and the final position after surgical correction of the patient’s spine.

This aspect of the project, although providing qualitative rather than quantitative results, has greatly benefited the surgeons assessing the results of the instrumentation. Not only are they able to watch the simulated surgical correction dynamically, but they are able to see it from different points of view and from dynamic points of view. The commercial model does not detract from the accuracy of the animation because the curvature of the spine is what is wanted – the shape of the individual vertebrae is not as important as the change in the shape of the spine.

By integrating our software with a commercial software package for modeling and motion control, it was easy to produce “professional quality” animated visualizations for real-time preview or off-line rendering and post production. One advantage of this approach is that as new releases of the animation software become available we can easily add more realistic rendering effects that might otherwise require significant implementation effort on our part.

4.4 Multi-user Extensions

Our more recent work has been examining multi-user extensions that permit network-based collaboration in the viewing and analysis of data utilizing high-speed ATM (asynchronous transfer mode) communication links.

Again, we have taken advantage of commercial software that provides shared 2-D screens and video teleconferencing to provide some of the support. But we have added some custom in-house software that shares viewing and pointing control between two workstations, both displaying local copies of the same model, but utilizing control information shared across the network.

We expect that a number of commercial software packages will provide this capability in the near future (some are already available). We have developed our own special-purpose software for this application as an interim measure to guarantee real-time response. The availability of ATM network connections between our computer graphics laboratory at the University of British Columbia and a number of the affiliated research hospitals has given us the opportunity to experiment with our prototype 3-D collaborative software and to develop strategies for future network-based tools for use in the scoliosis studies.

The advantages of working over a network, instead of having to travel between sites, has made a significant difference in our ability to conduct the research. We expect this experience to lead us to develop more tools for collaborative telemedicine including some planned uses in clinical health care delivery now underway.

5 DISCUSSION

We believe that the research that is using our new visualization tools will lead to better and more cost-effective health care treatment. Improvements in the quality of health care can be expected as a result of the better understanding

of scoliosis gained through these studies. Reduction in the cost of health care will result from better treatment by appropriate design and use of surgical instrumentation and by earlier detection and intervention in severe cases.

The original spinal instrumentation system, the Harrington system, has been widely abandoned in scoliosis surgery in favour of segmental instrumentation systems, such as the Moss-Miami system currently used at B.C. Children's Hospital. However, there is ongoing debate whether expensive systems such as these really provide any better correction than the less expensive Harrington system. The application of these systems has been largely empirical. Operative planning often is based on the surgeon's previous experience, but not on specific measured criteria. Until now, no accurate system has been able to assess vertebral correction in three dimensions. Stereophotogrammetry allows for three-dimensional assessment and has the added advantage of measuring the results of specific intraoperative maneuvers independently.

These techniques can provide two types of benefits. First, the accurate measurement of the results of spinal instrumentation surgery will allow the indications for specific instrumentation systems to be clearly defined, thus minimizing unnecessary use of complex instrumentation systems in cases where they provide no improvement in outcome. Second, instrumentation placement can be more precisely planned, thus maximizing the correction of the scoliotic deformity in each patient, and improving the results of the surgery. An example of this can be seen in the assessment of the plane of maximum deformity that our study provides. The plane of maximum deformity should be corrected to equal that of a normal spine. Although good correction of the plane is observed in some patients, in others it is poor, and no clear reason for this has been given in the literature. Comparison of the plane corrections achieved by different instrumentation application patterns will allow the optimum pattern to be selected.

6 REFERENCES

1. Andre, B., et al., "Effects of Radiographic Landmark Identification Errors on the Accuracy of Three Dimensional Reconstruction of the Human Spine", *Medical and Biological Engineering and Computing*, pp. 569-575, Nov 1992.

2. Beauchamp, A., Dansereau, J., de Guise, J., Labelle, H., "Computer assisted digitization system for scoliotic spinal stereo radiographs", *International symposium on 3-D scoliotic deformities*, Montreal, Canada, June 1991.
3. Benson, D.R., Shultz, A.B., Dewald, R.I., "Roentgenographic evaluation of vertebral rotation" *JBJS* 58-A, p. 1125, 1976.
4. Burt P.J., Yen C., Xu X., "Local Correlation Measures for Motion Analysis: A comparative study," *Proc. IEEE Conf. Pattern Recognition Image Processing*, pp. 269-274, 1982.
5. Cobb, J.R., "Outline for the Study of Scoliosis", *Instructional Course Lectures, the American Academy of Orthopaedic Surgeons*, Vol 5, Ann Arbor, MI, J.W. Edwards Co., pp. 261-275, 1948.
6. De Smet A.A., et al., "A Radiographic Method for Three- Dimensional Analysis of Spinal Configuration", *Diagnostic Radiology*, 137, pp. 343-347, 1980.
7. Efron, Bradley, *The Jackknife, the Bootstrap, and Other Resampling Plans*, Philadelphia: Society of Industrial and Applied Mathematics, 1982.
8. Golub, G.H., Van Loan, C.H., *Matrix Computations*, Baltimore: John Hopkins University Press, pp. 425-426, 1983.
9. Leon, Steven J., *Linear Algebra with Applications*, 2nd Ed., New York: MacMillan Publishing Company, 1986.
10. Russell, G.G., et al., "A Comparison of Four Computerized Methods for measuring Vertebral rotation", *Spine* 15 (1) 1990.
11. Transfeld, E., et al., "Three Dimensional Changes in the Spine Following Cotrel-Dubousset Instrumentation for Adolescent Idiopathic Scoliosis", *6th Cotrel-Dubousset Instrumentation*, pp. 73-79, 1989.
12. Wolf, Paul R., *Elements of Photogrammetry*, McGraw-Hill Book Company, 1974.

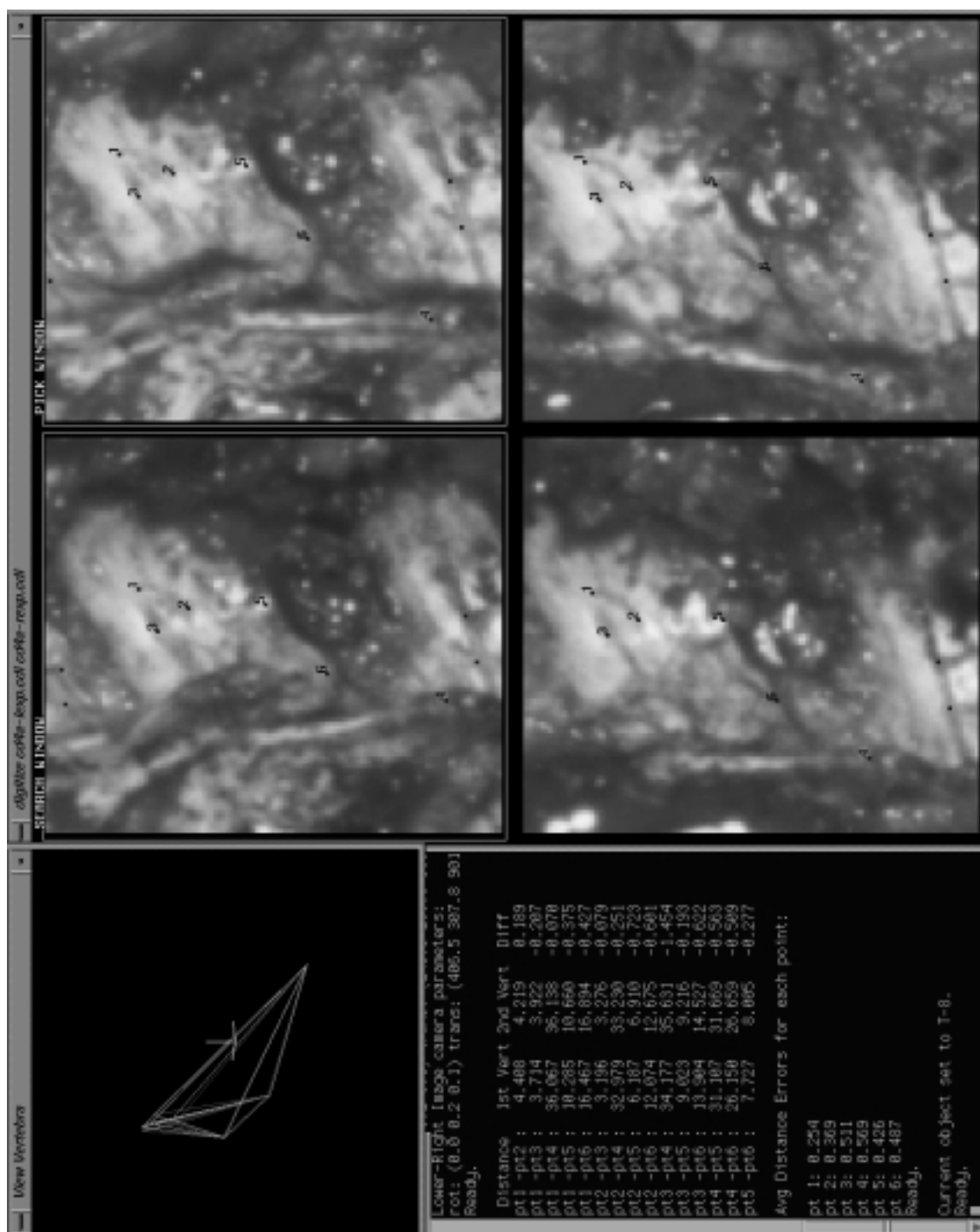


Figure 2: A screen dump of the stereo digitization software. The landmarks for the current vertebra, T-8, are numbered 1 to 6, in each of the four sub-images. On the upper-left of the screen is a 3-D wire-frame representation of T-8's data. On the lower-right is the console window that displays information about the software and the vertebral data.



Figure 3: A 3-D wire-frame representation of the data from the first (darker objects) and last (lighter objects) stages of a case. The vertebrae that the data represent are T-5 to T-11. Digitized points on the same vertebra are connected by straight line segments.